

Supporting Information

**[Zn(H<sub>2</sub>O)<sub>4</sub>][Zn<sub>2</sub>Sn<sub>3</sub>Se<sub>9</sub>(MeNH<sub>2</sub>)]: A robust open framework chalcogenide with large non linear optical response**

Manolis J. Manos,<sup>a</sup> Joon I. Jang,<sup>b</sup> John B. Ketterson<sup>b</sup> and Mercouri G. Kanatzidis \*<sup>a</sup>

<sup>a</sup> Department of Chemistry, 2145 Sheridan Road, Northwestern University, Evanston, IL 60208-3113, USA. E-mail:

m-kanatzidis@northwestern.edu; Fax: 847-491-593; Phone: 847-467-1541

<sup>b</sup>Department of Physics and Astronomy, Northwestern University, Evanston, IL 60208-3113, USA

**Powder X-ray Diffraction (PXRD).** The samples were examined by X-ray powder diffraction for identification purposes and to assess phase purity. Powder patterns were obtained using a CPS 120 INEL X-ray powder diffractometer with Ni-filtered Cu K $\alpha$  radiation operating at 40 kV and 20 mA and equipped with a position-sensitive detector. Samples were ground and spread on a glass slide. The purity of phases was confirmed by comparison of the X-ray powder diffraction patterns to ones calculated from single crystal data using the NIST Visualize 1.0.1.2 software.

**Inductively Coupled Plasma-Atomic Emission (Optical Emission)/Mass Spectroscopy [ICP-AES(OES)/MS] analyses.** The determination of the content of Sn, Zn and Se of compound (**1**) was performed on diluted aqua regia (HCl:HNO<sub>3</sub> = 3:1) solutions of (**1**) by ICP-AES using VISTA MPX CCD SIMULTANEOUS ICP-OES instrument. Standards of the ions of interest were prepared by diluted commercial (Aldrich or GFS chemicals) ~1000 ppm ICP-standards of these ions. The calibration was linear with error of 5 %. The samples were also diluted before the measurements, so that their concentrations can fall within the range of calibration. The ICP-AES intensity was the result of three (30 seconds) exposures. For each sample, three readings of the ICP-AES intensity were recorded and averaged. The standards were reanalyzed after analysis of the samples.

**EDS analyses.** The analyses were performed using a JEOL JSM-6400V scanning electron microscope (SEM) equipped with a Tracor Northern energy dispersive spectroscopy (EDS) detector. Data acquisition was performed with an accelerating voltage of 25 kV and 40 s accumulation time.

**IR spectroscopy.** Infrared spectra (IR) in the mid-IR region [4000-400 cm<sup>-1</sup>, Diffuse Reflectance Infrared Fourier Transform (DRIFT) method] were recorded with a computer-controlled Nicolet 750 Magna-IR series II spectrometer equipped with a TGS/PE detector and silicon beam splitter in 2-cm<sup>-1</sup> resolution.

**Thermal Analysis.** Thermogravimetric analysis (TGA) was carried out with a Shimatzu TGA 50. Samples (10±0.5 mg) were placed in aluminum crucible. Samples were heated from ambient

temperature to 600 °C in a 20 ml/min flow of N<sub>2</sub> or air. Heating rate of 10 °C/min was used and continuous records of sample temperature, sample weight and its first derivative (DTG) were taken.

**Proton ion-exchange experiment.** A typical ion-exchange experiment of compound (**1**) with proton ions is as follows: Compound (**1**) (0.04 mmol, 54 mg) was added as a solid in 20 mL HCl (6 M) solution. The mixture was kept under magnetic stirring for ≈ 12 h. Then, the red polycrystalline material was isolated by filtration, washed several times with water, acetone and ether and dried in air. Yield ~ 30 mg.

**Nonlinear Optic Property Measurement.** We use the frequency-tripled output of a passive-active mode-locked Nd:YAG laser with a pulse width of about 15 ps and a repetition rate of 10 Hz to pump an optical parametric amplifier (OPA). The OPA generates vertically polarized pulses in the ranges 400 ~ 685 nm and 737 ~ 3156 nm. In order to check the SHG efficiency as a function of the excitation energy, we tune the wavelength of the incident light from 1200- 2000 nm. In this range, the spectral bandwidth of the linearly polarized light from the OPA is rather broad, about 2 meV full width at half maximum. However, the phase space compression phenomena ensures effective SHG where lower energy portions are exactly compensated by higher parts thereby satisfying both energy and momentum conservation. The incident laser pulse of 300 μJ was focused onto a spot 500 μm in diameter using a 3 cm focal-length lens. The corresponding incident photon flux is about 10 GW/cm<sup>2</sup>. The SHG signal is collected in a reflection geometry from the excitation surface and focused onto a fiber optic bundle. The output of the fiber optic bundle is coupled to the entrance slit of a Spex Spec-One 500 M spectrometer and detected using a nitrogen-cooled CCD camera. The data collection time is 20 s.

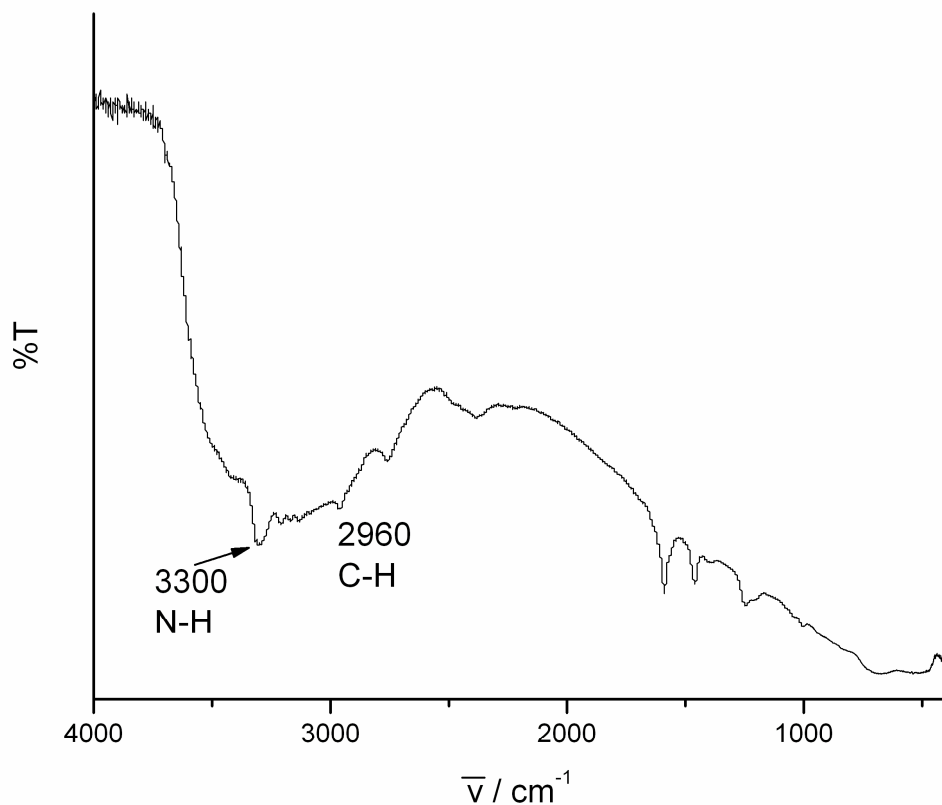


**Fig. S1.** Mid-IR spectrum of compound (1) with the assignment of some characteristic methylamine absorptions.

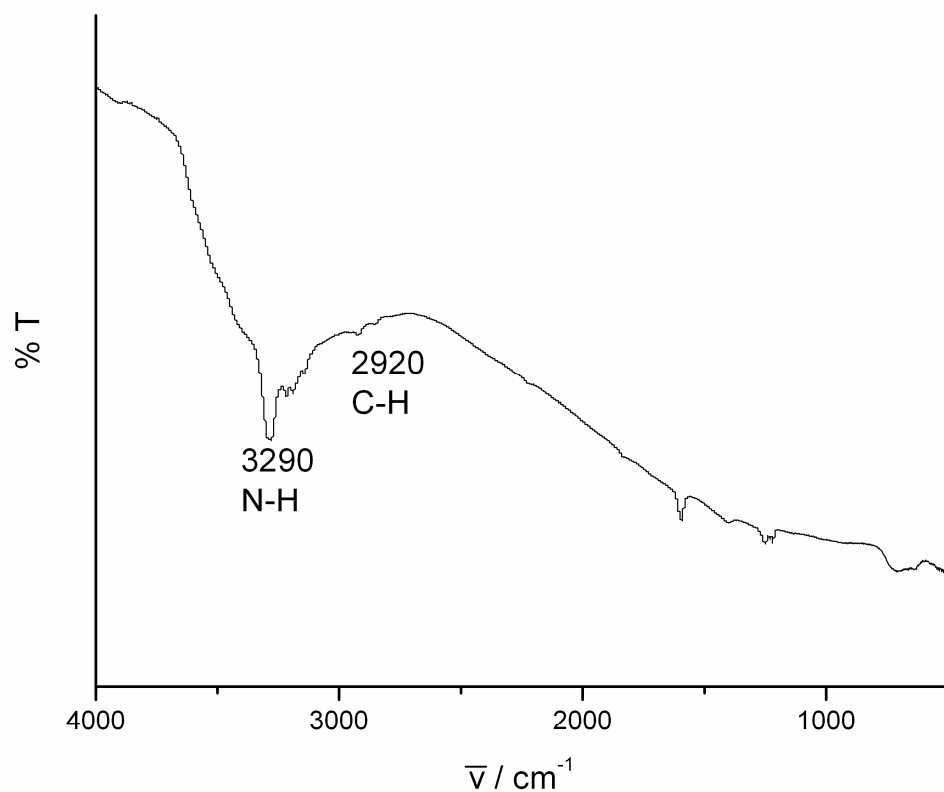


**Fig. S2.** Mid-IR spectrum of the proton-exchanged analogue of (**1**) with the assignment of some characteristic methylamine absorptions.

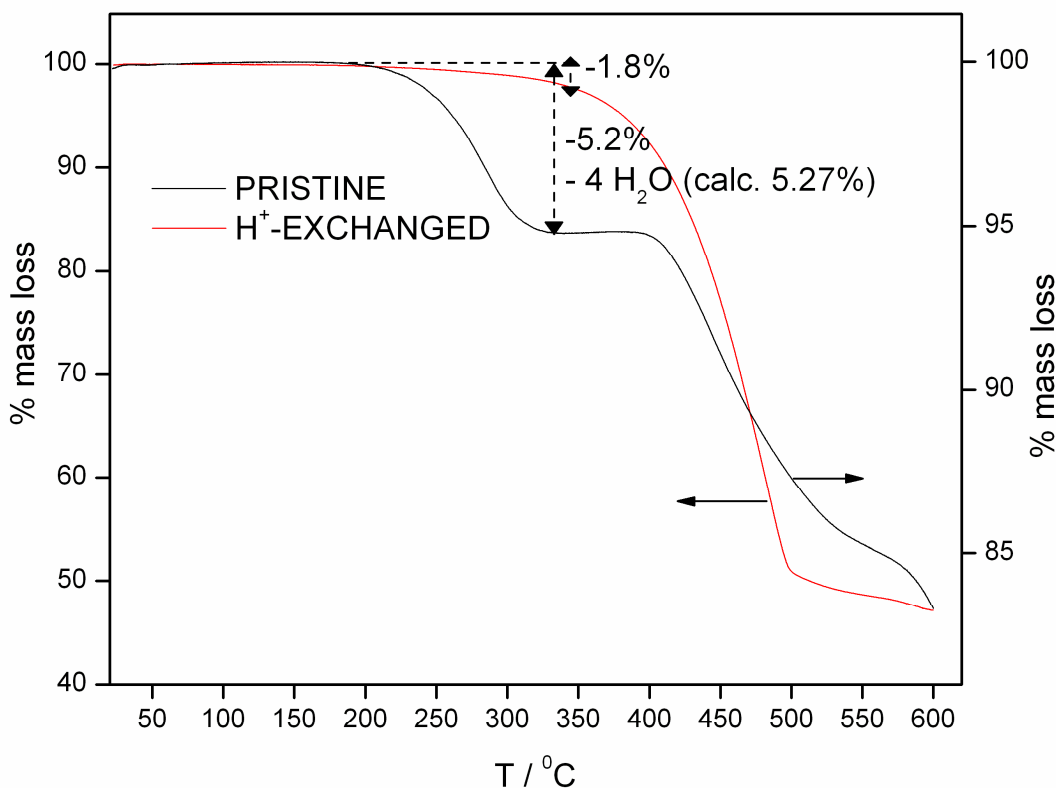
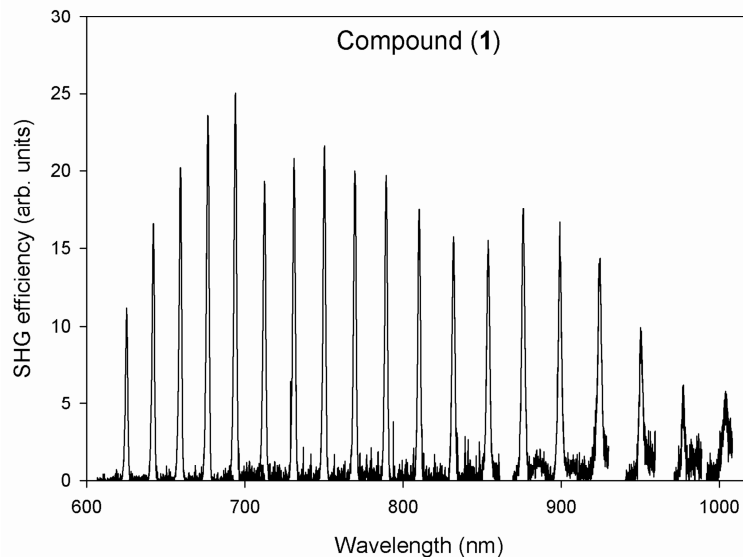


**Fig. S3.** TGA curves for the pristine compound (**1**) and its proton-exchanged analogue. Negligible mass loss was observed from 25 to 200 °C for both materials. The mass loss of ~ 5.20 % for compound (**1**) till 330 °C is assigned as removal of 4 water molecules (calculated water mass loss based on the  $[\text{Zn}(\text{H}_2\text{O})_4][\text{Zn}_2\text{Sn}_3\text{Se}_9(\text{MeNH}_2)]$  formula is 5.27 %). It seems that the methylamine is released along with selenium atoms during the second step of mass loss (after 400 °C). The water content seems to be substantially reduced after the proton exchange of (**1**), since the mass loss of the proton-exchanged analogue till 330 °C is only 1.8 %. The total mass losses (~ 600 °C) for the pristine and proton-exchanged materials were 16.7 % and 52.9 % respectively. The higher instability of the proton-exchanged compound may be due to the presence of the proton ions that facilitate the removal of selenium as H<sub>2</sub>Se.

(a)



(b)

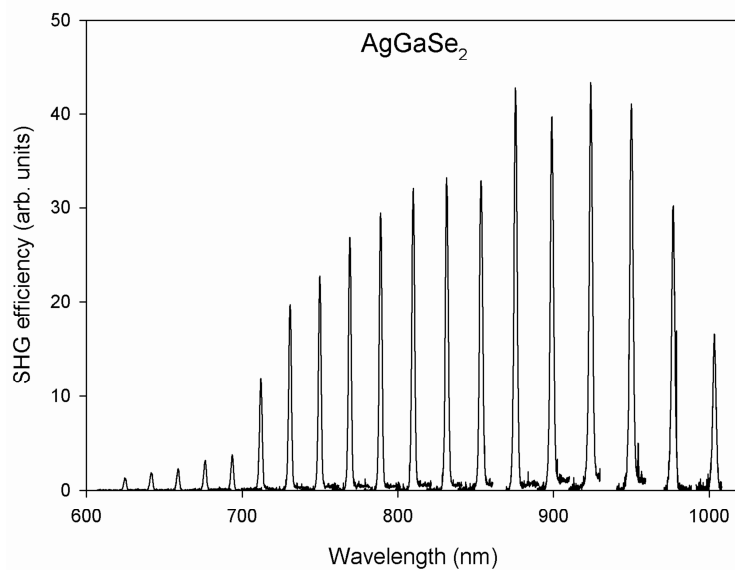


**Fig. S4.** (a) SHG efficiency of compound (1) versus the wavelength of the SHG signal. (b) SHG efficiency of  $\text{AgGaSe}_2$  versus the wavelength of the SHG signal. The maximum SHG efficiency ( $\sim 25$ ) for compound (1) corresponding to 694 nm is  $\sim 58\%$  of the maximum SHG efficiency ( $\sim 43$ ) of  $\text{AgGaSe}_2$  corresponding to  $\sim 924$  nm. The particle size range used for both compound (1) and  $\text{AgGaSe}_2$  was 45–63  $\mu\text{m}$ .